**M.N. Taran**, DrSc (Geology, Mineralogy), Senior Research Fellow, Head of Department
M.P. Semenenko Institute of Geochemistry, Mineralogy and Ore Formation of the NAS of Ukraine
34, Acad. Palladin Ave., Kyiv, Ukraine, 03142
E-mail: m_taran@hotmail.com; https://orcid.org/0000-0001-7757-8829

# SYNTHETIC CO-EXISTING WADSLEYITE β-(Mg, Fe)$_2$SiO$_4$ AND RINGWOODITE γ-(Mg, Fe)$_2$SiO$_4$: AN OPTICAL ABSORPTION SPECTROSCOPY STUDY

*The synthetic high-pressure α- and β-modification of $(Mg_{1-x}Fe_x)_2SiO_4$, wadsleyite and ringwoodite, respectively, were studied by optical absorption spectroscopy at ambient and hydrostatic high-pressure conditions. In addition, the effects of thermal annealing on the crystals were investigated. Under hydrostatic compression up to ~13 GPa and then consequent released to atmospheric pressure there were changes in the spectra and related changes in the crystal color. This is a clear indication that some $Fe^{2+}$ was oxidized to $Fe^{3+}$. The spectra of both ringwoodite and wadsleyite change after annealing in air at temperatures up to 300 °C. The intensities of electronic spin-allowed bands of $Fe^{2+}$ decrease and the intensity of the charge-transfer electronic transition $O^{2-} \rightarrow Fe^{3+}$, as given by the low-energy absorption edge in the UV region, increases. These crystal-chemical changes are shown by a weakening of the blue (ringwoodite) and green (wadsleyite) colors and a concomitant increase in yellowish tints. The effects of $Fe^{2+}$ oxidation to $Fe^{3+}$, upon decompression from high pressures as well as through annealing at relatively low temperatures, can cause the disintegration of both phases. Thus, both minerals have not yet been reliably identified at near surface Earth conditions after originating from deep-seated volcanism or deep subduction zone processes.*

***Keywords:*** *ringwoodite, wadsleyite, optical absorption spectra, influence of temperature and pressure.*

**Introduction.** Iron, mostly as Fe$^{2+}$ and, at lesser extent, as Fe$^{3+}$, is believed to be the most abundant transition metal component of all three (Mg, Fe)$_2$SiO$_4$ polymorphs, olivine (α), wadsleyite (β) and ringwoodite (γ), both substituting Mg in the octahedral sites of the structure. In nearly all mantle olivines found in deep-seated xenoliths [e.g., 3] or as micro-inclusions in diamonds [e.g., 18], the total Fe-content calculated to fayalite component is close to Fa10, while the contents of other transition metals are orders of magnitude lower. Wadsleyite and ringwoodite, abundant, as believed, in the transition zone of the Earth, are also assumed to have a bulk chemical composition similar to the upper mantle olivine, i.e. (Mg$_{1-x}$Fe$_x$)$_2$SiO$_4$ with $x \approx 0.1$ [12]. Note that iron admixture may appreciably influence the sound velocities, single-crystal elastic properties of wadsleyite and ringwoodite

[13], as well as their radioactive thermal conductivity [8, 25].

Up to now, ringwoodite of terrestrial origin was found as remnants of extremely small dimension in lithospheric mantle materials that, as assumed, was initially subducted into the transition zone and later re-exhumed to the seafloor [7]. As microscopic inclusion, it was found in a diamond from Juína, Brazil [13]. Ringwoodite of impact genesis was identified as microscopic particles of a few micrometers long in pumice of the El Gasco Area, Western Spain [6].

By now only synthetic ringwoodite and wadsleyite and, in lesser extent, those of meteoritic origin are applicable for spectroscopic studies. Optical absorption spectroscopy is an important part of such investigations [8, 21, 20, 25, 11]. Still, very little is known about pressure (*P*) and temperature
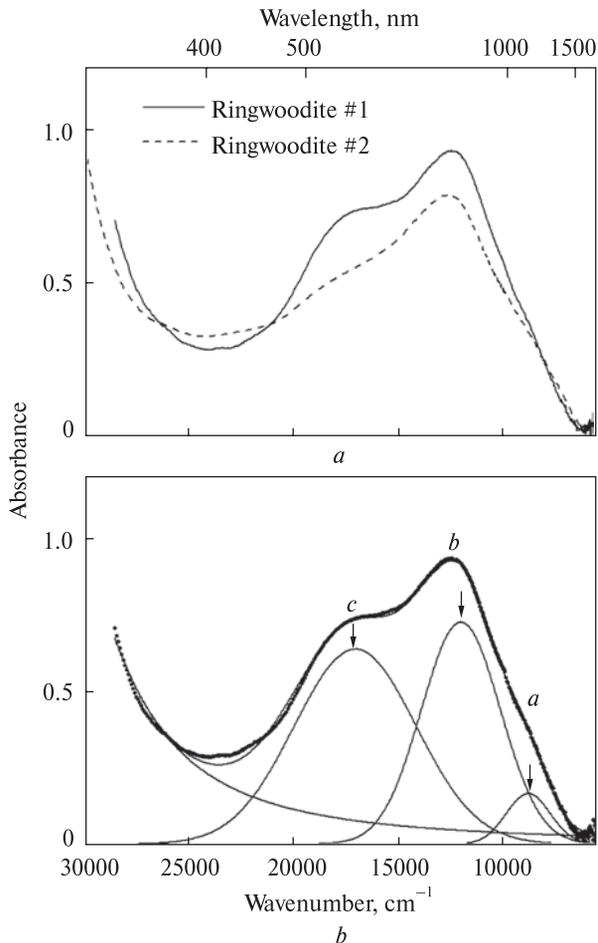
*Fig. 1.* Optical absorption spectra of two ringwoodite grains studied, #1 and #2, measured at ambient conditions (*a*); result of the curve fitting analysis of the sample #1 (*b*). The high-energy absorption edge, approximated by a sum of the Gauss and Lorentz functions, and three broad absorption bands *a*, *b* and *c*, approximated by the Gauss functions, are main spectroscopic features of the spectrum

**Experimental section.** Co-existing wadsleyite and ringwoodite (run MA-305) were synthesized at 16.7 GPa and 1200 °C in a multi-anvil apparatus for 24 h. A stoichiometric mixture of FeO, MgO and $SiO_2$ oxides were used as starting material [20]. Microprobe analysis gave averaged composition $(Mg_{0.92}Fe_{0.08})_2SiO_4$ for wadsleyite and $(Mg_{0.85}Fe_{0.15})_2SiO_4$ for ringwoodite thus showing an appreciable preference of iron for ringwoodite.

By very distinct difference in colors, green of wadsleyite and blue of ringwoodite, as well as by contrast behavior between crossed polarizers, several transparent grains of each phase around 100 μm in diameter were picked up from the grained run product at visual observation in scattered transmittance illumination in a binocular microscope. From two grains of differently saturated blue color, a darker ringwoodite #1 and a lighter ringwoodite #2, two polished on both sides platelets around 50 μm thick were prepared for optical absorption spectroscopy study. As the ringwoodite structure is of cubic symmetry, the orientation of the platelets was of no importance. In case of wadsleyite, which structure belongs to the orthorhombic system, two oriented sections of thickness ~50 μm, allowing measuring spectra in E∥X-, E∥Y- and E∥Z-polarization, were prepared from two similarly colored dark-green grains. The orientation of the platelets was controlled by conoscopic observation in polarizing microscope.

Optical absorption spectra in the range 330—1800 nm (ca. 30303—5560 $cm^{-1}$) at ambient and high-pressure conditions were measured on a home-made single-beam microspectrophotometer described elsewhere [24]. Optical absorption spectra were fitted by Gaussian components using Peakfit 4.11 software. The high-energy absorption edge was taken as a sum of Gaussian and Lorentzian curves.

**Results and discussion.** *Ringwoodite.* Optical absorption spectra of two ringwoodite samples, #1 and #2, measured at ambient condition, together with the result of the curve-fitting analysis of the former, are shown in Fig. 1, *a* and *b*, respectively.

(*T*) effects on optical absorption spectra of these phases. In this work the co-existing synthetic Fe-bearing wadsleyite and ringwoodite are investigated by optical absorption spectroscopy at different pressures. The effects of compression-decompression and thermal annealing on the spectra were studied as well.

**Results of curve fitting in the energy range 30,000—5,555 $cm^{-1}$ of the spectrum of synthetic ringwoodite MA-305 at ambient conditions (cf. Fig. 1, *b*). FWHM (or half-width) is full band width at half maximum height**

| Band | Energy, $cm^{-1}$ | Linear intensity, $\log(I_o/I)$ | Linear absorption coefficient $1/d \cdot \log(I_o/I)$, $cm^{-1}$ | FWHM, $cm^{-1}$ |
|------|------|------|------|------|
| *a* | 8,900 | 0.16 | 32 | 2,483 |
| *b* | 12,110 | 0.72 | 144 | 4,433 |
| *c* | 17,140 | 0.63 | 126 | 6,833 |

As seen, the main components, visually discernable and derived by the curve fitting procedure, are a high-energy absorption edge and three broad bands, $a$, $b$ and $c$. Spectroscopic parameters of $a$-, $b$- and $c$-band are compiled in Table.

The spectra closely remind those of the blue synthetic ringwoodite of similar iron contents, studied in [8, 11]. The parameter of $a$-, $b$- and $c$-band at ambient $P$ and $T$, i.e. energies of the peaks, intensity ratio and half-widths (Table 1), are fairly consistent with the same name bands in Table 3 of [8], where bands $a$ and $b$ are assigned to the split spin-allowed electronic $^5T_{2g} \rightarrow {}^5E_g$ transition of $^{VI}Fe^{2+}$ and band $c$ to $Fe^{3+}/Fe^{2+}$ IVCT transition between the ions in neighboring edge-sharing octahedral sites of the ringwoodite structure. On the other hand, as seen from Tab. 1, by energy these bands appreciably differ from the $a$-, $b$- and $c$-bands in spectra of high-iron ($X_{Fe} = 0.50$) bluish-green ringwoodite MA-68 (Table 3 in [21]), also assigned as the spin-allowed $dd$-bands of $^{VI}Fe^{2+}$ and $Fe^{3+}/Fe^{2+}$ IVCT band, respectively. These differences are most probably caused by different iron content. At least the difference in energies of the spin-allowed dd-bands of $^{VI}Fe^{2+}$, $a$ and $b$, may be caused by the concentration shift, typical for many Mg-Fe-bearing silicates [1].

The distinct difference in the intensity ratio of bands $a$- and $b$- vs. $c$-band in ringwoodites #1 and #2 (Fig. 1, $a$), undoubtedly evidences that band $c$ belongs to an absorption center different from that of $a$ and $b$: the deduction, which is consistent with the above-cited attributions. As the absorption edge is most likely the tail of extremely intense UV band(s), caused by electronic oxygen-metal charge transfer transitions mainly of $O^{2-} \rightarrow Fe^{3+}$ type [21, 11], this implies that iron in ringwoodites #1, 2, studied here, is less oxidized than in MA-68, studied in [21]. Then, the series of relatively weak and narrow bands $d$, $e$ and $f$ at ~19140, ~19850 and ~21740 $cm^{-1}$, observed in the latter work, should also be caused by $Fe^{3+}$. As to the most prominent band at 21740 $cm^{-1}$ this assumption is in a good consistency with the results of thermally induced oxidation of synthetic low-iron ($X_{Fe} \cong 0.10$) ringwoodite MA313 [11], where its appearance and intensification together with enhancement of the absorption edge and color change from blue to orange at annealing in air up to 600 °C is very prominent. Note that a weak band at ~21740 $cm^{-1}$ appeared also in spectrum of ringwoodite #1, undergone to annealing in air in processes of consequent measuring of spectra at temperatures 100, 200 and 300 °C (see below).
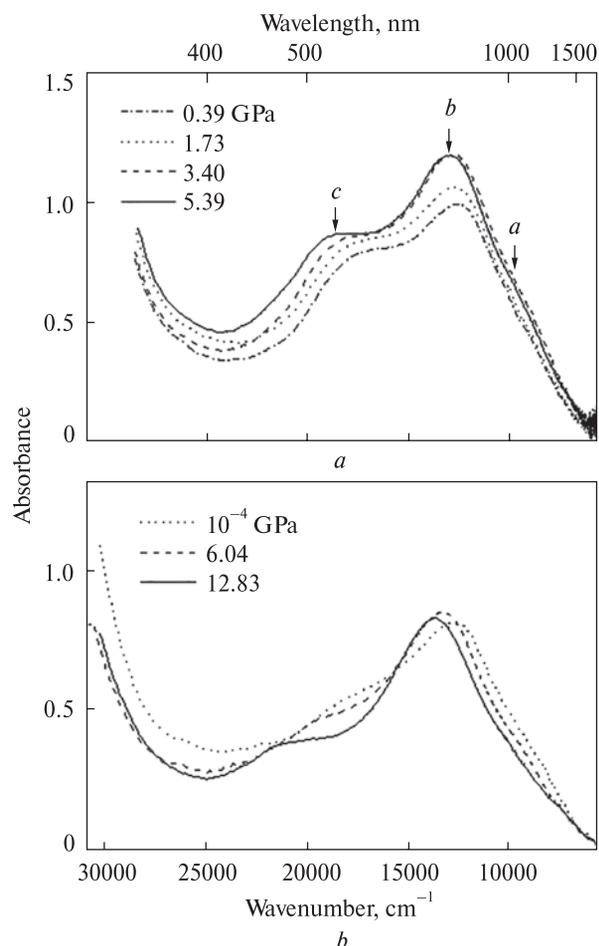


Fig. 2. High-pressure absorption spectra of two ringwoodites: $a$ — ringwoodite #1; $b$ — ringwoodite #2

High-pressure spectra of ringwoodite #1 in the range $10^{-4}$ — 5.39 GPa are shown in Fig. 2, $a$ and three representative spectra of the ringwoodite #2, measured at ambient pressure ($10^{-4}$ GPa), 6.04 GPa and 12.83 GPa, are shown in Figure 2, $b$.

Energies of $b$- and $c$-bands, derived by the curve-fitting procedure, vs. pressure are shown in Fig. 3. As seen, at increasing pressure both bands, $b$ and $c$, linearly shift to higher energies, but with nearly two times different rates: $\Delta v/\Delta P \approx$ ~123 $cm^{-1}$ $GPa^{-1}$ and ~217 $cm^{-1}$ $GPa^{-1}$, respectively. Besides, in the pressure range from atmospheric ($10^{-4}$ GPa) to ca. 3.5 GPa the band $b$ somewhat increases in intensity (Fig. 2, $a$), while that of the $c$-band remains practically unchanged up to the highest pressure achieved. The position of $a$-band is not so certain because of its strong overlapping with much more intense and broader band $b$ (cf. Fig. 1, $b$). Nevertheless, it looks like as under the pressure $a$-band shifts to higher energies either.

Therefore, one may reasonably conclude that the pressure-induced behaviours of bands $a$ and $b$
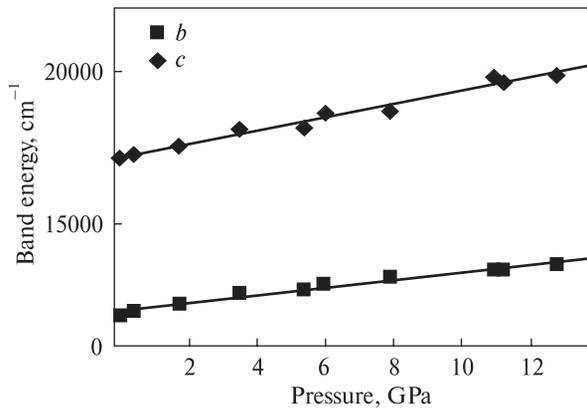
Fig. 3. Energy of the absorption bands *b* and *c* vs. pressure in ringwoodite evaluated by the curve fitting procedure. The solid lines are linear approximation of the experimental data described by equations $\nu = 12220 + 123 \cdot P$ (band *b*) and $\nu = 17176 + 217 \cdot P$ (band *c*). The correlation coefficient R equals 0.98164 and 0.98610, respectively. It should be noted that a polynomial fit of $\nu = A + B_1 \cdot P + B_2 \cdot P^2$ type gives better values of R for band *b*, 0.99519, but worse for band *c*, 0.97283
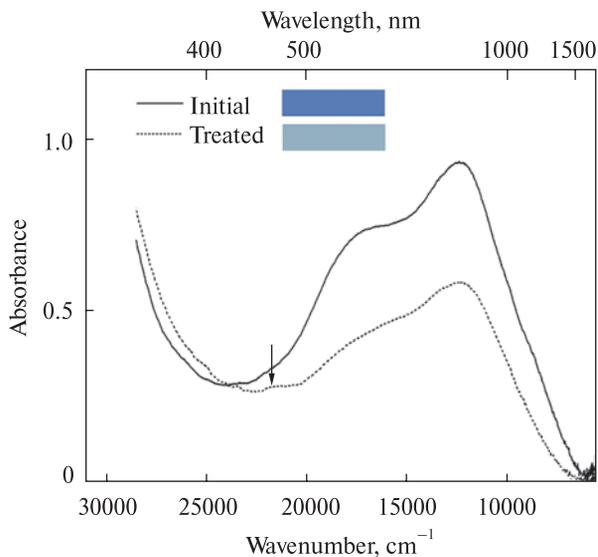


Fig. 4. Optical absorption spectra of ringwoodite #1 before and after stepwise measuring of high-temperature spectra at 100, 200 and 300 °C (see text). The weak band at ~21740 cm$^{-1}$ indicates increased amount of Fe$^{3+}$ in the annealed sample comparing with the initial one. The colored labels display the HTML colors (HTML colors are colors which can be reproduced by modern computer monitors. They are commonly used in websites and other software applications. There are a variety of formats, including Hex color codes and HTML color names. Particularly, the Hex colors codes can be calculated from color coordinates of the CIE colorimetric system XYZ, which, in turn, are calculated from optical spectra of materials), calculated from the spectra measured at the actual thickness of the sample for illumination by transmitting polarized light of the standard CIE illuminant C

are rather typical for the spin-allowed *dd*-bands of Fe$^{2+}$ partly undergone by an exchange-coupled interaction with neighboring Fe$^{3+}$ [cf. 23].

The band *c*, which energy and half-width at ambient pressure (Table 1) are consistent with its assignment to Fe$^{3+}$/Fe$^{2+}$ IVCT band [e.g. 10, 1, 19], shows much stronger *P*-induced shift to higher energy than in spectra of other Fe$^{2+}$, Fe$^{3+}$-bearing minerals studied so far. Evidently, the main effect of hydrostatic compression is shortening of interatomic distances of structure, including the distance between neighboring Fe$^{2+}$ and Fe$^{3+}$ involved into the IVCT process. At first sight this should lead rather to decrease of energy of IVCT transition, than to increase of it. This circumstance was duly remarked by Keppler and Smyth [8], who also detected an unusually strong pressure-induced blue-shift of the band ($\Delta\nu/\Delta P \approx 126$ cm$^{-1}$ GPa$^{-1}$, as could be calculated from Tab. 2 of the referred paper). They assumed that an important circumstance may be the fact that O-O distances in shared and unshared edges of the adjacent octahedral sites of the ringwoodite structure are somewhat different. This difference may increase with pressure, increasing the energy barrier for electronic charge-transfer transition between Fe$^{2+}$ and Fe$^{3+}$ ions and, thus, the energy of it. Such explanation reminds the deduction of Khomenko and Platonov [9], who on a set of natural amphiboles showed that common O-O distance in octahedral Fe$^{2+}$- and Fe$^{3+}$-centered edge-sharing sites significantly contributes to strength of charge-transfer potential barrier and, thus, to energy of Fe$^{2+}$/Fe$^{3+}$ IVCT band. It can hardly be added anything more to such argumentations. Note, however, that none of the theoretical considerations [26, 2, 5, 14] derived any dependence of energy of IVCT transition on donor-acceptor distance or any other dimensional factor.

Also, I cannot find any plausible explanation of the fact that in the high-iron ringwoodite MA-62 of $(Mg_{0.39}Fe_{0.61})_2SiO_4$ composition, studied in [21], the rate of pressure-induced shift of *c*-band is significantly lower, almost none, compared with that in ringwoodite of $(Mg_{0.85}Fe_{0.15})_2SiO_4$ composition, studied here, ~217 cm$^{-1}$ GPa$^{-1}$. Still, in ringwoodite of appreciably lower iron content, $(Mg_{0.90}Fe_{0.10})_2SiO_4$, studied in work [8], the rate is much weaker, ~126 cm$^{-1}$ GPa$^{-1}$, than that found in the present work.

Having in mind that from the transition metals only iron is present in appreciable amount in ringwoodites studied here, one has to admit the

$Fe^{2+}/Fe^{3+}$ IVCT nature of the *c*-band despite the strong dependence of its energy on pressure, strongly differing from other $Fe^{2+}$, $Fe^{3+}$-bearing minerals, studied so far [e.g. 19]. By this characteristic, it profoundly differs from the *c*-band in MA-62 ringwoodite of $(Mg_{0.39}Fe_{0.61})_2SiO_4$ composition, also assigned to electronic $Fe^{2+}/Fe^{3+}$ IVCT transition [21].

To clarify the nature of the *c*-band we tried to measure optical absorption spectra of the sample #1 at elevated temperatures to reveal a response of band's intensity to temperature, which in spectra of other $Fe^{2+}$, $Fe^{3+}$-bearing minerals is very strong and characteristic [e.g. 16, 15, 22, 19]. However, all attempts gave an uncertain result that very likely is due to a continual concurrent change of spectroscopic characteristics of the sample during the measurements at elevated temperatures applied, 100, 200 and 300 °C. Indeed, the visual effect after the stepwise heating at the high-temperature spectroscopic measurements was a clearly perceivable fading of the blue color of the sample and appearance of greenish component in it. We compared the spectra of the sample before and after the consequent heating at 100, 200 and 300 °C in the high-temperature spectroscopy experiments (Fig. 4). Following the results [11] on synthetic ringwoodite MA313, $[Mg_{0.86(1)}Fe^{2+}_{0.10(1)}Fe^{3+}_{0.01(1)}]_2Si_{0.95(1)}H_{0.31(4)}O_4$, such thermal treatment caused a distinct decrease of intensity of all three *a*-, *b*- and *c*-absorption bands and the increase (shift) of the absorption edge. The *c*-band decreased stronger than the bands *a* and *b*, again indicating the different nature of the former vs. the latter.

The decrease of *a*- and *b*-bands, attributed to spin-allowed dd-transition of $^{VI}Fe^{2+}$, evidences of a considerable oxidation of $Fe^{2+}$ to $Fe^{3+}$. A weak band at ~21740 $cm^{-1}$, marked in the Fig. 4 by arrow, which appeared in spectrum at annealing in air in processes of consequent measuring of spectra at temperatures 100, 200 and 300 °C, also evidences of $Fe^{2+}$ to $Fe^{3+}$oxidation. The concomitant increase (shift) of the absorption edge to lower energy and appearance of band at ~21740 $cm^{-1}$, is consistent with such interpretation and is in a good agreement with the results by Mrosko et al. [11].

Another observation, which looks very strange and unexpected, is that the influence of pressure on spectrum of both ringwoodite samples, #1 and #2, is not entirely reversible, since the intensities of *a*-, *b*- and *c*-bands in spectra of both samples, #1 and #2, released from hydrostatic compression, are appreciably weaker than in the initial ones. On the
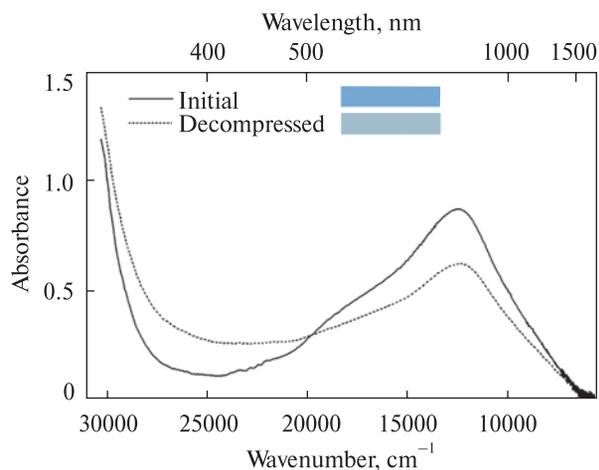


*Fig. 5.* Optical absorption spectra of ringwoodite #2, the initial and after step by step compressing to 12.83 GPa and decompressed to ambient pressure. The colored labels are the same as in Fig. 4

contrary, the high-energy edge evidently increases (shifts to lower energies). These are well seen in Fig. 5, where the spectra of ringwoodite #2, initial and released after stepwise compressing to 12.83 GPa (cf. Fig. 2, *b*) to atmospheric pressure, are shown.

Note that the strength of such effect depends on the highest pressure achieved at compression: in ringwoodite #1, compressed to only 5.39 GPa, it is much weaker, than in #2, compressed to 12.83 GPa. In fact, the influence of pressure (or pressure release, or both compression and pressure release) on optical absorption spectrum reminds the effect of thermal annealing (cf. Figs. 4 and 5) and evidences that both actions cause significant iron oxidation in ringwoodite. To the best of our knowledge, such compression-decompression effect was never described before (at least in minerals). On the contrary, Frank and Drickamer [4], for instance, described the effect of pressure-induced reduction of iron in some chemical compounds. On this account they assumed that in Earth depths iron in minerals exists predominantly in form of $Fe^{2+}$.

It is also worth mentioning that under release of pressure microscopic cracks appeared in the samples, their amount and intensity definitely depending on maximal pressure applied: in ringwoodite #1, compressed to only 5.39 GPa, there were much less amount of them and they were weaker and less discernible than in #2, compressed to 12.8 GPa). It is not yet clear whether these two effects caused by hydrostatic pressure, oxidation of $Fe^{2+}$ and fracture damage to specimens by cracks, are related to each other. However, why we cannot surmise that very
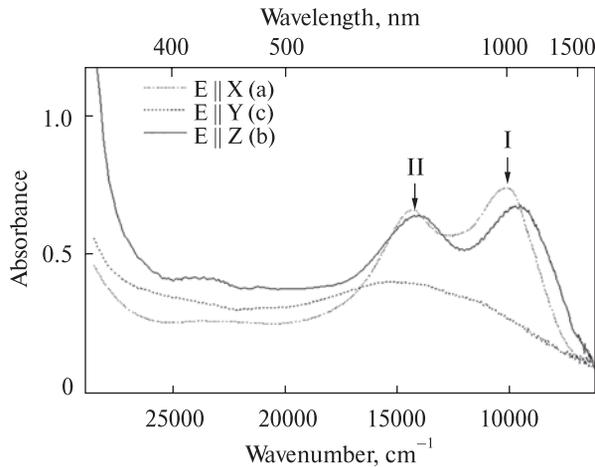
Fig. 6. Polarized optical absorption spectra of synthetic $(Mg_{0.92}Fe_{0.08})_2SiO_4$ wadsleyite
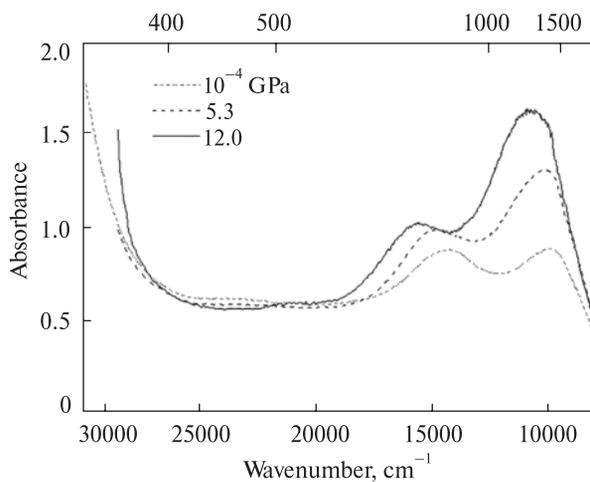


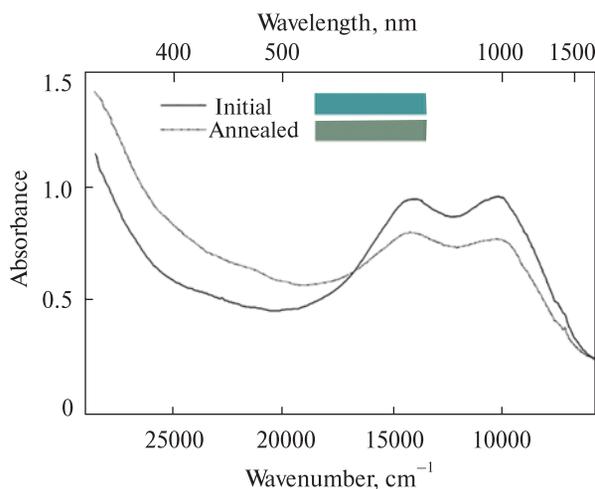Fig. 7. High-pressure spectra of wadsleyite



Fig. 8. Unpolarized spectra of wadsleyite before and after annealing in air at 300 °C during 1 hour. The colored labels as in Fig. 4

poor, almost none, representation of ringwoodites of terrestrial origin, is related to such extraordinary behavior of ringwoodite at pressure release? Indeed, if oxidized $Fe^{3+}$-rich ringwoodite is less stable than $Fe^{2+}$-rich one, the easy oxidation $Fe^{2+}$ to $Fe^{3+}$ at annealing and, especially, at decompression, which, in addition, is accompanied by cracking of ringwoodite grains, may be the cause of disintegration of this phase at elevating from the depth by mechanisms of kimberlitic volcanism [13] or plate tectonics [7]. Obviously, temperature- and pressure-induced oxidation of $Fe^{2+}$ to $Fe^{3+}$ in the ringwoodite structure needs some charge compensating mechanism. Taking into consideration that in synthetic samples there is always some amount of hydroxyl groups, the charge compensation is most probably provided over lost of protons by the scheme $Fe^{2+} + OH^- \rightarrow Fe^{3+} + O^{2-} + \frac{1}{2} H_2$ [11, 12].

*Wadsleyite.* The polarized spectrum of wadsleyite is shown in Fig. 6. In near infrared range it is rather similar to that of synthetic hydrous wadsleyite II with 0.18 apfu Fe, studied by [17]. The spectrum consists of a high-energy absorption edge and two broad intense bands at ~9700 $cm^{-1}$ (band I) and ~14000 $cm^{-1}$ (band II), both strong in E‖X- and E‖Z-polarizations.

From comparison with the results of [17] one may conclude that in wadsleyite, which in difference to cubic ringwoodite belongs to orthorhombic system, the orientation is X‖a, Y‖c and Z‖b. By energy, ~9700 $cm^{-1}$, and half-width, ~3500 $cm^{-1}$, the band I is typical spin-allowed *dd* transition of octahedrally coordinated $Fe^{2+}$. In this respect the band II is similar to electronic $Fe^{2+}/Fe^{3+}$ IVCT transition between iron ions in the adjacent octahedral sites. On the other hand, its half-width, ~4200 $cm^{-1}$, is too low comparing with other minerals showing electronic $Fe^{2+}/Fe^{3+}$ IVCT transitions, e.g. [1]. That can evidence in favor of its electronic spin-allowed dd-transition nature. As there is no indication of narrow band at 470 nm (21 280 $cm^{-1}$) which appears in all three polarization of the spectrum reported by [17] and which is, very probably, caused by $Fe^{3+}$ (spin-forbidden transition $^6A_{1g} \rightarrow {}^4A_{1g}, {}^4E_g$), one may conclude that our sample is comparatively weakly oxidized.

As seen from unpolarized spectra measured at different pressures (Fig. 7), hydrostatic compression causes shifts of the both bands, I and II, to higher energies ($\Delta\nu/\Delta P \approx 70$ $cm^{-1}$/GPa and 110 $cm^{-1}$/GPa, respectively) that again indicates, as stated above, that both are most likely caused by

electronic spin-allowed *dd*-transitions in octahedral $Fe^{2+}$. Similar to a- and b-bands in ringwoodite (see above), the lower energy band I strongly increases in intensity that evidence of its intensification over exchange interaction with neighboring $Fe^{3+}$ [23]. Contrary to ringwoodite no indication of cracking at decompression was observed in case of wadsleyite.

As can be seen from the comparison of unpolarized spectra measured before and after annealing in air at 300 °C during ca. one hour (Fig. 8), the absorption bands I and II are thermally unstable, both showing a noticeable decrease in intensity.

That is accompanied by intensification or a "red-shift" of the high-energy absorption edge. Visually the sample changes its color from bluish-green to green, as it is displayed in the Figure 8 by the HTML colors, calculated from the spectra measured before and after the treatment. In this respect the thermal behaviour of wadsleyite closely resembles that of ringwoodite. That is caused by a significant oxidation of $Fe^{2+}$ to $Fe^{3+}$ in the octahedral positions of the structure.

**Conclusions.** Optical absorption spectroscopy evidences that in synthetic ringwoodite and wadsleyite $Fe^{2+}$ partly oxidizes to $Fe^{3+}$ at relatively low temperatures ~300 °C. In ringwoodite, $Fe^{2+}$-oxidation is also generated by the processes of hydrostatic compression (to ~13 GPa) and subsequent decompression to ambient pressure. Besides, the process of decompression is accompanied by appearance of numerous microscopic cracks in the sample, which amount and size depend on value of maximal pressure, achieved at compression. It is assumed that the observed effects of $Fe^{2+}$ to $Fe^{3+}$ oxidation at annealing and compression-decompression and appearance of microscopic cracks in ringwoodite at decompression may promote a decay of ringwoodite and wadsleyite at their elevation in processes of plates tectonics or deep-seated kimberlitic volcanism and thus be the reason of an extreme scarcity of these minerals of terrestrial origin.

REFERENCES

1. Burns, R.G. (1993), *Mineralogical Applications of Crystal Field Theory*, 2nd ed., Cambridge Univ. Press, Cambridge, 576 p.
2. Cox, P.A. (1980), *Chem. Phys. Letters,* Vol. 69, No. 2, pp. 340-343. https://doi.org/10.1016/0009-2614(80)85076-7
3. Deer, W.A., Howie, R.A. and Zussman, J. (1997), *Rock forming minerals: orthosilicates,* 2nd ed., Geological Society of London, London.
4. Frank, C.W. and Drickamer, H.G. (1976), *The Physics and Chemistry of Minerals and Rocks,* in Strens, R.G.J. (ed.), Wiley, New York, pp. 509-544.
5. Girerd, J.J. (1983), *J. Chem. Phys.,* Vol. 79, No. 4, pp. 1766-1775. https://doi.org/10.1063/1.446021
6. Glazovskaya, L.I. and Feldman, V.I. (2012), *Petrology,* Vol. 20, No. 5, pp. 415-426. https://doi.org/10.1134/S0869591112050049
7. Griffin, W.L., Afonso, J.C., Belousova, E.A., Gain, S.E., Gong, X.-H., González-Jiménez, J.M., Howell, D., Huang, J.-X., McGowan, N., Pearson, N.J., Satsukawa, T., Shi, R., Williams, P., Xiong, Q., Yang, J.-S., Zhang, M. and O'Reilly, S. (2016), *J. Petrol.,* Vol. 57, No. 4, pp. 655-684. https://doi.org/10.1093/petrology/egw011
8. Keppler, H. and Smyth, R.J. (2005), *Amer. Mineral.,* Vol. 90, No. 7, pp. 1209-1212. https://doi.org/10.2138/am.2005.1908
9. Khomenko, V.M. and Platonov, A.N. (1996), *Phys. Chem. Minerals,* Vol. 23, No. 4, pp. 243. https://doi.org/10.1007/BF00207761
10. Mattson, S.M. and Rossman, G.R. (1987), *Phys. Chem. Minerals,* Vol. 14, No. 1, pp. 94-99. https://doi.org/10.1007/BF00311152
11. Mrosko, M., Lenz, S., McCammon, C.A., Taran, M., Wirth, R. and Koch-Müller, M. (2013), *Amer. Mineral.,* Vol. 98, No. 4, pp. 629-636. https://doi.org/10.2138/am.2013.4245
12. Núñez-Valdez, M., da Silveira, P. and Wentzcovitch, R.M. (2011), *J. Geophys. Res.,* Vol. 116, No. B12, p. B12207. https://doi.org/10.1029/2011JB008378
13. Pearson, D.G., Brenker, F.E., Nestola, F., McNeill, J., Nasdala, L., Hutchison, M.T., Matveev, S., Mather, K., Silversmit, G., Schmitz, S., Vekemans, B. and Vincze, L. (2014), *Nature,* Vol. 507, pp. 221-224. https://doi.org/10.1038/nature13080
14. Sherman, D.M. (1987), *Phys. Chem. Minerals,* Vol. 14, No. 4, pp. 355-363. https://doi.org/10.1007/BF00309810

15. Smith, G. (1977), *Canad. Mineral.,* Vol. 15, No. 4, pp. 500-507.

16. Smith, G. and Strens, R.G.J. (1976), *The Physics and Chemistry of Minerals and Rocks,* in Strens, R.G.J. (ed.), Wiley, New York, pp. 583-612.

17. Smyth, J.R., Holl, C.M., Langenhorst, F., Laustsen, H.M.S., Rossman, G.R., Kleppe, A., McCammon, C.A., Kawamoto, T. and van Aken, P.A. (2005), *Phys. Chem. Minerals,* Vol. 31, No. 10, pp. 691-705. https://doi.org/10.1007/s00269-004-0431-x

18. Sobolev, N.V., Logvinova, A.M., Zedgenizov, D.A., Pokhilenko, N.P., Kuzmin, D.V. and Sobolev, A. (2008), *Eur. J. Miner.*, Vol. 20, No. 3, pp. 305-315. https://doi.org/10.1127/0935-1221/2008/0020-1829

19. Taran, M.M. (2020), *Optical spectroscopy of ions of transition metals of minerals at different temperatures and pressures: spectroscopic, crystal chemical and thermodynamic aspects,* Nauk. dumka, Kyiv, UA, 400 p. (in Ukrainian).

20. Taran, M.N. and Koch-Müller, M. (2012), *14th Int. Conf. Experimental Mineralogy, Petrology, Geochemistry EMPG, 03-06.03.2012,* Kiel, Germany, Abstracts, p. 136.

21. Taran, M.N., Koch-Müller, M., Wirth, R., Abs-Wurmbach, I., Rhede, D. and Greshake, A. (2009), *Phys. Chem. Minerals,* Vol. 36, No. 4, pp. 217-232. https://doi.org/10.1007/s00269-008-0271-1

22. Taran, M.N. and Langer, K. (1998), *Neues Jb. Miner. Abh.,* Band 172, Heft 2-3, pp. 325-346. https://doi.org/10.1127/njma/172/1998/325

23. Taran, M.N., Langer, K. and Platonov, A.N. (1996), *Phys. Chem. Minerals,* Vol. 23, No. 4-5, pp. 230-236. https://doi.org/10.1007/BF00207754

24. Taran, M.N., Ohashi, H. and Koch-Müller, M. (2008), *Phys. Chem. Minerals*, Vol. 35, No. 3, pp. 117-127. https://doi.org/10.1007/s00269-007-0202-6

25. Thomas, S.-M., Bina, C.R., Jacobsen, S.D. and Goncharov, A.F. (2012), *Earth and Planet. Sci. Lett.*, Vol. 357-358, No. 1, pp. 130-136. https://doi.org/10.1016/j.epsl.2012.09.035

26. Wong, K.Y., Schatz, P.N. and Piepo, S.B. (1979), *J. Amer. Chem. Soc.*, Vol. 101, No. 11, pp. 2793-2803. https://doi.org/10.1021/ja00505a001

*М.М. Таран,* д-р геол.-мін. наук, старш. наук. співроб., зав. від.
Інститут геохімії, мінералогії та рудоутворення ім. М.П. Семененка НАН України
03142, м. Київ, Україна, пр-т Акад. Палладіна, 34
E-mail: m_taran@hotmail.com; https://orcid.org/0000-0001-7757-8829

ШТУЧНІ СПІВІСНУЮЧІ ВАДСЛЕІТ β-(Mg, Fe)$_2$SiO$_4$ І РИНГВУДИТ
γ-(Mg, Fe)$_2$SiO$_4$: ОПТИКО-СПЕКТРОСКОПІЧНЕ ДОСЛІДЖЕННЯ

Вивчено штучно вирощені високобаричні α- і β-модифікації олівіну складу (Mg$_{1-x}$Fe$_x$)$_2$SiO$_4$, вадслеіт і рингвудит, відповідно, за допомогою методу оптичної спектроскопії за звичайних умов і за високих гідростатичних тисків. Також вивчено вплив на кристали термічного прожарювання. У разі рингвудиту встановлено, що гідростатичне стиснення до ~13 ГПа і наступна декомпресія спричинюють зміни в оптичних спектрах і, внаслідок, у характері забарвлення, що є явною ознакою того, що частина іонів Fe$^{2+}$ окиснюється до Fe$^{3+}$. Спектри як рингвудиту, так і вадслеіту змінюються і внаслідок прожарювання обох мінералів на повітрі за температури до 300 °C. Інтенсивність дозволених за спіном смуг Fe$^{2+}$ зменшується, а інтенсивність смуг переносу заряду O$^{2-}$ → Fe$^{3+}$, представлена в спектрах у вигляді краю УФ-поглинання, зростає. Ці кристалохімічні зміни видно як ослаблення синього (рингвудит) і зеленого (вадслеіт) забарвлення і супутнього підсилення водночас жовтуватих відтінків. Ефекти окиснення Fe$^{2+}$ до Fe$^{3+}$ у ході декомпресії, а також під час прожарювання за відносно низьких температур можуть бути причиною руйнування указаних фаз в процесах їхнього виносу із перехідної зони в процесах глибинного кімберлітового вулканізму або внаслідок підйому (ексгумації) рингвудит- і вадслеітвмісних порід із зон субдукції. Унаслідок ці мінерали земного генезису надійно ще не встановлено.

*Ключові слова*: рингвудит, вадслеіт, оптичні спектри, вплив температури і тиску.